SIERRA Mechanics for Coupled Multi-Physics Modeling of Salt Repository Behavior for NEAMS Applications

SAND2011-6761C

J. Guadalupe Argüello and J. S. Rath
Computational Structural Mechanics & Applications Department, Sandia National Laboratories, Albuquerque, NM 87185-0372, USA

Proposed for publication in the conference proceedings of "SaltMech7 – 7th Conference on the Mechanical Behavior of Salt," to be held at MINES ParisTech from April 16-20, 2012 in Paris, France.

ABSTRACT: The Nuclear Energy Advanced Modeling & Simulation (NEAMS) Waste Integrated Performance & Safety Code (IPSC) project is tasked to develop the "next-generation" of computational tools to model nuclear waste repositories in order to quantitatively assess the long-term performance of a disposal (or a storage) system in an engineered/geologic environment. To achieve this goal, the Waste IPSC will incorporate three levels of model fidelity: constitutive relationships derived from mechanistic sub-continuum processes; high-fidelity continuum models; and moderate-fidelity Performance Assessment (PA) continuum models. The integration of modeling and simulation capabilities at these three levels of fidelity will derive from a combination of existing code acquisition and new code development. An effort on high-fidelity continuum modeling was undertaken to exercise the existing SIERRA Mechanics code suite. A series of simulations and their results will be presented and discussed herein to illustrate some of the capabilities available in SIERRA Mechanics for simulating salt repositories.

1 INTRODUCTION

The goal of the Nuclear Energy Advanced Modeling & Simulation (NEAMS) Waste Integrated Performance & Safety Code (IPSC) project is to develop the "next-generation" of computational tools to model nuclear waste repositories through an integrated suite of multi-physics computational modeling and simulation capabilities to quantitatively assess the long-term performance of a disposal (or storage) system in an engineered/geologic environment (Freeze et al. 2010, Freeze et al. 2011). The Waste IPSC will provide this simulation capability for a range of disposal concepts including various waste form types, engineered barrier designs, and geologic settings; for a range of temporal and spatial scales; with appropriate consideration of the associated uncertainties; and in accordance with rigorous verification, validation, and software quality requirements.

To achieve this goal, the Waste IPSC will incorporate three levels of model fidelity: constitutive relationships derived from mechanistic sub-continuum processes; high-fidelity continuum models; and moderate-fidelity Performance Assessment (PA) continuum models.

The integration of modeling and simulation capabilities at these three levels of fidelity will derive from a combination of existing code acquisition and new code development. These multi-fidelity modeling and simulation capabilities must be supported by efficient software frameworks and enabling tools/infrastructure, also derived from a combination of existing and new computer codes. Toward this end, a preliminary validation effort on high-fidelity continuum modeling was undertaken using the SIERRA Mechanics suite of codes developed by Sandia National Laboratories (Edwards & Stewart 2001) to exercise and evaluate the code suite for applicability to this class of problems.

The development of the SIERRA Mechanics code suite has been funded by the USA Department of Energy (DOE) Advanced Simulation and Computing (ASC) program for more than ten years. The goal is development of massively parallel multiphysics capabilities to support the Sandia engineering sciences mission. SIERRA Mechanics was designed and developed from its inception to run on the latest and most sophisticated, massively parallel computing hardware. It has the capability to span the hardware range from a single workstation to computer systems with thousands of processors. The foundation of SIERRA Mechanics is the SIERRA toolkit, which provides finite element application-code services such as: mesh and field data management, both parallel and distributed; transfer operators for mapping field variables from one mechanics application to another; a solution controller for code

coupling; and included third party libraries (e.g., solver libraries, communications package, etc.). The SIERRA Mechanics code suite is comprised of application codes that address specific physics regimes. The two SIERRA Mechanics codes that are used as the launching point for fully integrated Thermal-Hydrological-Mechanical-Chemical (THMC) coupling, with adaptive solution control, in a repository-setting are Aria (Notz et al. 2007) and Adagio (SIERRA Solid Mechanics Team 2010).

The physics currently supported by Aria include: the incompressible Navier-Stokes equations, energy transport equation, and species transport equations, as well as generalized scalar, vector, and tensor transport equations. A multi-phase porous flow capability has been recently added to Aria. Aria also has basic geochemistry functionality available through embedded chemistry packages.

The mechanics portion of the THMC coupling is handled by Adagio. It solves for the quasi-static, large deformation, large strain behavior of nonlinear solids in three dimensions. Adagio has some discriminating Sandia-developed technology for solving solid mechanics problems, that involves matrix-free iterative solution algorithms for efficient solution of extremely large and highly nonlinear problems. This technology is especially well-suited for scalable implementation on massively parallel computers. The THMC coupling is done through a solution controller within SIERRA Mechanics called Arpeggio.

In this work we describe the application of the SIERRA Mechanics code suite to a set of salt repository problems recently exercised to validate its applicability to this class of problems and to demonstrate its use on anticipated more-complex coupled simulations of future nuclear waste salt repositories. We describe its use on the following problems of interest: the simulation of the isothermal WIPP Mining Development Test (Room D) Thermal/Structural Interactions in-situ experiment (Munson et al. 1988); the simulation of the WIPP Overtest for Simulated Defense High-Level Waste (Room B) Thermal/Structural Interactions in-situ experiment (Munson et al. 1990b); and another recent simulation of a generic salt repository for high-level waste (Stone et al. 2010). Results from the various simulations will be presented and discussed to illustrate the capabilities available in SIERRA Mechanics for simulating salt repositories.

2 DESCRIPTION OF AND RESULTS FOR WIPP CONFIGURATIONS

Several large-scale in-situ tests were fielded underground at the Waste Isolation Pilot Plant (WIPP) during an early phase of its development. The expressed purpose of these in-situ tests was to provide the database for validation of the predictive technology that was being developed at the time for use in the licensing process (Matalucci et al. 1982). Among the pieces of the validation technology being developed then was the Multi-mechanism Deformation (MD) creep constitutive model that was eventually adopted by WIPP. The MD model, which has been migrated to and is available in the current SIERRA Mechanics toolset, will first be presented in this section. The WIPP Room D and Room B Thermal/Structural Interactions in-situ test configurations and the computational models that were used in this work are then described and results for those calculations are presented. Rooms B and D were chosen because they were located in the same general location within the WIPP and at the same horizon, with the major difference between them being that Room D was at ambient conditions while Room B was subjected to a significant thermal load via heaters in the floor.

2.1 *Multi-mechanism deformation (MD) constitutive creep model*

The Multi-mechanism Deformation (MD) creep model originally developed by Munson & Dawson (1979, 1982, & 1984) and later extended by Munson et al. (1989) was used in these analyses. The MD model mathematically represents the primary and secondary creep behavior of salt due to dislocations under relatively low temperatures (compared to the melting temperature) and low to moderate stresses which are typical of mining and storage cavern operations. Three micromechanical mechanisms, determined from deformation mechanism maps (Munson 1979), are represented in the model: a dislocation climb mechanism active at high temperatures and low stresses; an empirically observed mechanism active at low temperatures and low stresses; and a dislocation slip mechanism active at high stresses. These creep mechanisms are assumed to act such that the total steady state creep rate can be written as the sum of the individual mechanism strain rates.

$$\dot{\varepsilon}_s = \sum_{i=1}^{3} \dot{\varepsilon}_{s_i} \tag{1}$$

The influence of temperature on the creep strain rate is included through an Arrhenius term. The steady state creep strain rates for the first and second mechanisms are identical in form and are implemented using a power law model while the third mechanism (dislocation slip) is represented using an Eyring type model.

$$\dot{\varepsilon}_{s_1} = A_1 \left(\frac{\sigma_{eq}}{G} \right)^{n_1} e^{\frac{-Q_1}{RT}} \tag{2}$$

$$\dot{\varepsilon}_{s_2} = A_2 \left(\frac{\sigma_{eq}}{G} \right)^{n_2} e^{\frac{-Q_2}{RT}} \tag{3}$$

$$\dot{\varepsilon}_{s_3} = \left(B_1 e^{-Q_1/RT} + B_2 e^{-Q_2/RT} \right) \sinh\left[q \left(\frac{\sigma_{eq} - \sigma_0}{G} \right) \right] \times H\left(\sigma_{eq} - \sigma_0\right) \tag{4}$$

where σ_{eq} is the equivalent stress; T is the temperature (absolute); G is the shear modulus; A_1, A_2, B_1, & B_2 are structure factors; Q_1 & Q_2 are activation energies; R is the universal gas constant; q is the activation volume, σ_0 is the stress limit; and H is the Heaviside function with argument $(\sigma_{eq} - \sigma_0)$.

From the definition of the Heaviside function, the third mechanism is only active when the equivalent stress exceeds the specified value of the stress limit σ_0. The equivalent stress appearing in these equations is taken to be the Tresca stress (Munson, et al. 1989). The Tresca stress can be written in terms of the maximum and minimum principal stresses σ_1 and σ_3 respectively ($\sigma_1 \geq \sigma_2 \geq \sigma_3$). Alternatively, the Tresca stress may be written as a function of the Lode angle, ψ, and the second invariant, J_2, of the deviatoric stress tensor, **s** (with components s_{ij}).

$$\sigma_{eq} = \sigma_1 - \sigma_3 = 2\cos\psi\sqrt{J_2} \tag{5}$$

The Lode angle is dependent on both the second and third invariant, J_3, of the deviatoric stress tensor, s_{ij}.

$$\psi = \frac{1}{3}\sin^{-1}\left[\frac{-3\sqrt{3}J_3}{2J_2^{3/2}} \right] \qquad -\frac{\pi}{6} \leq \psi \leq \frac{\pi}{6} \tag{6}$$

$$J_2 = \frac{1}{2} s_{ij} s_{ji} \tag{7}$$

$$J_3 = \frac{1}{3} s_{ij} s_{jk} s_{ki} \tag{8}$$

The kinetic equation used in the MD model is given by Equation 9 where F is a function which accounts for transient creep effects and $\dot{\varepsilon}_s$ is the steady state dislocation creep strain rate defined by Equation 1.

$$\dot{\varepsilon}_{eq} = F \dot{\varepsilon}_s \tag{9}$$

The function F has three branches: a work hardening branch (F > 1), an equilibrium branch (F = 1), and a recovery branch (F < 1).

$$F = \begin{cases} \exp\left[\Delta \left(1 - \dfrac{\zeta}{\varepsilon_t^f} \right)^2 \right] & \zeta < \varepsilon_t^f \text{ Transient Branch} \\ 1 & \zeta = \varepsilon_t^f \text{ Equilibrium Branch} \\ \exp\left[-\delta \left(1 - \dfrac{\zeta}{\varepsilon_t^f} \right)^2 \right] & \zeta > \varepsilon_t^f \text{ Recovery Branch} \end{cases} \tag{10}$$

The choice of the particular branch depends on the transient strain limit ε_t^f and the internal variable ζ. The transient strain limit is defined by Equation 11 where K_0, c, and m are material parameters, T is the absolute temperature, and G is the shear modulus.

$$\varepsilon_t^f = K_0 e^{cT} \left(\frac{\sigma_{eq}}{G} \right)^m \tag{11}$$

The internal variable, ζ, appearing in the calculation of the function, F, is obtained by integration of the evolution equation

$$\dot{\zeta} = \left(F - 1\right) \dot{\varepsilon}_s \tag{12}$$

Δ and δ, appearing in Equation 10, are the work hardening and recovery parameters and are given by Equations 13 and 14 respectively. In these equations α, β, α_r, and β_r are material parameters. Typically the recovery parameter, δ, is taken to be constant (i.e. $\delta = \alpha_r$).

$$\Delta = \alpha + \beta \log\left(\frac{\sigma_{eq}}{\mu} \right) \tag{13}$$

$$\delta = \alpha_r + \beta_r \log\left(\frac{\sigma_{eq}}{\mu} \right) \tag{14}$$

If only the steady state creep response is of interest then the transient and recovery branches may be effectively turned off by setting $\alpha=0$, $\beta=0$, $\alpha_r=0$, $\beta_r=0$. The MD model can be further simplified to that of a power law creep model by setting the appropriate structure factors and activation energies to zero.

Including the bulk and shear moduli, which are both assumed constant, there are a total of 19 parameters used to define the MD model.

2.2 *Isothermal room configuration (Room D)*

2.2.1 *Test description and stratigraphy*

The isothermal WIPP Mining Development Test (Room D) consists of a test room set into the bedded stratigraphy of the natural salt formation. The room was constructed to be thermally and structurally isolated from the other test rooms by a large pillar, approximately 79 m thick. The room has a total length of 93.3 m. The test section of the room consists of the central 74.4 m of the room and has cross section dimensions of 5.5 m wide by 5.5 m high. The Room D coordinate center is at a depth, below the ground surface, of 646.0 m. Details of the mining of the room and of the measurements that were taken are given in Munson et al. (1988). The roof of Room D follows a parting defined by a small clay seam. This seam (Clay I), along with the rest of the clay seams, and the remainder of the stratigraphy around the

room are shown in Figure 1. This is the same stratigraphy used in the historical calculation of Munson et al. (1989), in which they reported agreement of the MD-model/SPECTROM-32 (2D) code combination with the Room D data. In this work, we attempted to duplicate the historical calculation as closely as possible with the MD-model/SIERRA toolset combination as an initial effort at validating SIERRA Mechanics for this class of problems.

The clay seams noted in the stratigraphy, according to Munson et al. (1989), are not in actuality distinct seams unless associated with an anhydrite layer but are rather local horizontal concentrations of disseminated clay stringers. Therefore, computationally, seam properties can be ascribed to the concentration of clay. In the calculational model of this work, as was also the case for the historical calculation, the clay seam shear response is specified by a coefficient of friction, μ=0.2. Of the thirteen clay seams labeled A through M, only the nine nearest the room labeled D through L are taken as active and included in the calculation.

2.2.2 *Configuration and computational model*

The calculational model represents a slice through the center of the room length and consists of a space defined by the vertical symmetry plane through the middle of the room and by a vertical far-field boundary placed far into the salt. So the model is effectively a plane strain model – which is appropriate for comparison with measurements taken at room mid-length for the relatively long room. Because the SIERRA mechanics toolset offers only a 3D capability, for the room calculations reported herein, the plane strain model is approximated by taking a slice (single element into the plane) to generate its 3D equivalent. The front and back faces of the resulting 3D model are then constrained against horizontal movement in the out-of-plane direction (Z-direction). The upper and lower extremes of the model are defined as shown. The boundaries, both vertical and horizontal, are sufficiently removed from the room that they cause an insignificant perturbation in stress or displacement at the room proper. Both of the vertical boundaries are constrained against horizontal (X-direction) movement, allowing only vertical displacements.

The horizontal boundaries are traction (lithostatic pressure) boundaries. A uniform pressure of 13.57 MPa is applied at the upper horizontal boundary, accounting for the weight of the overburden. Krieg (1984) determined the thickness weighted average of the densities of the materials in the layers of the calculational model yielding an average density in the model of 2.30 Mg/m^3. This density results in a uniform applied pressure of 15.97 MPa on the bottom horizontal boundary, and accounts for the presence of an instantaneously-mined room.

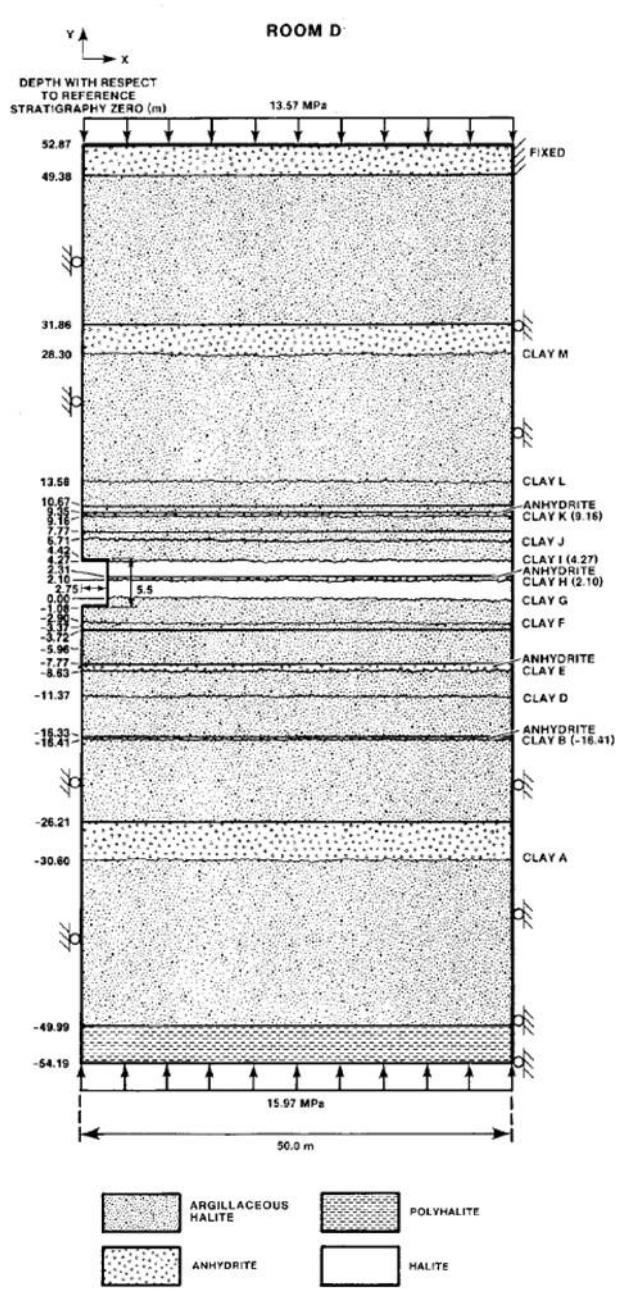

Figure 1. Local stratigraphy around and model of Room D.

A lithostatic initial stress state that varies linearly with depth is assumed, based on the average material density and a gravitational acceleration of 9.79 m/sec^2, in the model. The room surfaces are traction-free and the upper right corner of the calculational model is fixed against horizontal and vertical (X-Y) displacements.

Table 1. Parameter set used for Room D calculation.

	Parameters		Units	Halite
Elastic Properties	Shear modulus	G	MPa	12,400
	Young's modulus	E	MPa	31,000
	Poisson's ratio	ν	–	0.25

Salt Creep Properties	Structure Factors	A_1	s^{-1}	8.386×10^{22} (1.407×10^{23})
		B_1	s^{-1}	6.086×10^{6} (8.998×10^{6})
		A_2	s^{-1}	9.672×10^{12} (1.314×10^{13})
		B_2	s^{-1}	3.034×10^{-2} (4.289×10^{-2})
	Activation energies	Q_1	cal/mol	25,000
		Q_2	cal/mol	10,000
	Universal gas constant	R	cal/mol -^{o}K	1.987
	Absolute temperature	T	^{o}K	300
	Stress exponents	n_1	–	5.5
		n_2	–	5.0
	Stress limit of the dislocation slip mechanism	σ_0	MPa	20.57
	Stress constant	q	–	5,335
	Transient strain limit constants	M	–	3.0
		K_0	–	6.275×10^{5} (2.470×10^{6})
		c	$^{o}K^{-1}$	9.198×10^{-3}
	Constants for work-hardening parameter	α	–	-17.37 (-14.96)
		β	–	-7.738
	Recovery parameter	δ	–	0.58

The finite element mesh used in the SIERRA Mechanics calculation is not shown. However, it contains 2184 hexahedral elements and 5032 nodes.

2.2.3 *Closure results from SIERRA Mechanics*

The Room D simulation computed the first 1100 days of creep response of the room for comparison with the Room D measurements. The simulation used the above-described computational model and MD constitutive description, with the parameters for the MD model shown in Table 1. These parameter are identical to those given in Munson et al. 1989, in an effort to duplicate, as closely as possible, the historical calculation using SIERRA Mechanics in place of the earlier 2D SPECTROM-32 code. The parameters, shown in parenthesis in Table 1 under the "Halite" heading, are the parameters for argillaceous halite that are different from those for clean halite; most parameters are the same for the two materials that were used in the calculation.

Thus, it should be noted that the same assumptions that went into the historical calculation were also used in this one. For example, although the stratigraphy shows anhydrite and polyhalite layers, Munson et al. 1989 state: "Because these layers are either sufficiently thin to be insignificant in the calculational response or are sufficiently removed from the room being simulated to be quite un-influential in the calculational response, we did not include them in the calculation." Hence, the present SIERRA mechanics calculation did not include them either; instead the two materials were treated as argillaceous halite as was presumably done in the historical calculation.

It should also be noted that not all of the details of the historical calculations are well documented. Therefore, in those cases where those details are missing, we have made some assumptions, guided by expert judgment, to be able to repeat the historical calculation as closely as possible; as was the case above in treating the anhydrite and polyhalite layers as argillaceous halite rather than clean halite.

Figure 2 shows the room closure results from the mechanical simulation compared to the extensometer measurements of Room D closure. In view of the complexity of the calculation, the agreement between calculation and measurement is quite good, on the order of approximately 10% difference between them for both vertical and horizontal closure. This is of roughly the same order as the agreement seen in the historical calculation of Munson et al. (1989), and at least, in a preliminary sense, validates SIERRA Mechanics for isothermal conditions to roughly the same degree as was done for the code used in the historical calculation.

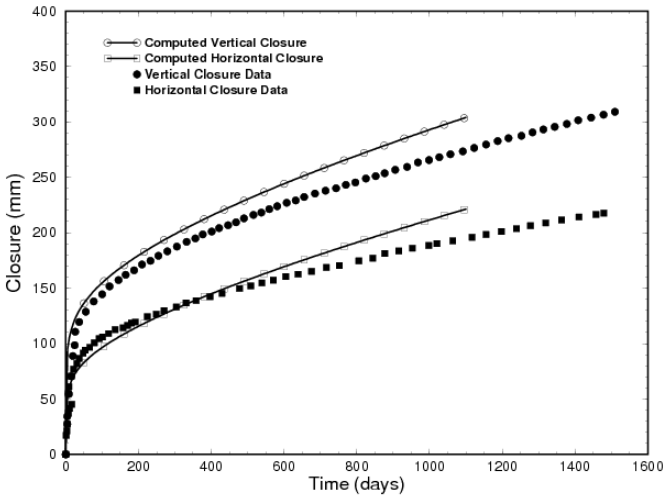

Figure 2. Comparison of calculated (SIERRA Mechanics) and measured in-situ Room D closures.

2.3 *Heated room configuration (Room B)*

2.3.1 *Test Description and Stratigraphy*

The WIPP Overtest for Simulated Defense High-Level Waste (Room B) Thermal/Structural Interactions in-situ experiment (Munson et al. 1990b) is another major thermal/structural test conducted at the WIPP. It consists of a long, 93.3 m, instrumented room with a square cross-section that is 5.5 m by 5.5 m. This room has electrically heated canisters that are 0.3 m diameter by 3.0 m long and placed, in evenly-spaced vertical boreholes that are

0.41 m diameter by 4.9 m deep, in the floor along the room centerline. These heaters, each with about 1.8kW of power, were placed on 1.52 m centers to give a linear heat load of 1.18 kW/m over the central 41.2 m of the room.

Closure and temperature measurements were made during the course of the experiment in the heavily-instrumented room. According to Munson et al. (1990a) closure measurements were made starting within one hour of the mining at that location and continued for the duration of the test. Three different thermocouple arrays were used to monitor the temperature conditions: one for monitoring the interior canister temperatures; another that monitored the temperatures in the vicinity of the canisters; and another that monitored the temperatures in the salt around the room. The test room operated in an unheated condition initially to give a baseline room response for comparison with other similar experimental rooms (including Room D) as well as to allow time for emplacement of the heaters and construction of insulated doors at the ends of the room.

Because creep of salt is a thermally-activated process, a modest increase in temperature produces a marked acceleration in room closure rate. Room B is of identical dimensions to Room D; is in the same general vicinity and at the same depth; and has the same stratigraphy (Fig. 1).

2.3.2 *Configuration and computational model*

The finite element calculations used to simulate the Room B in situ experiment consisted of two separate 3D models, a thermal model and a structural model. As discussed previously for Room D, a one-element through-the-thickness model was used to mimic the plane-strain 2D models in 3D. One-way coupling between the thermal and structural responses was employed; similar to what was performed in the historical calculation of Munson et al. (1990a) using the 2D thermal code SPECTROM-41 and 2D structural code SPECTROM-32, in an effort to duplicate the historical calculation as closely as possible. This one-way coupling implies that thermal response was assumed to be unaffected by structural deformations. The thermal model was used to compute temperatures in the geologic formation around Room B for a simulated period of five years. The SIERRA Mechanics thermal/fluids finite element code, Aria (Notz et al. 2007), was used for this calculation. The temperatures were then used as input to the SIERRA Mechanics structural finite element code, Adagio (SIERRA Solid Mechanics Team 2010), so that thermal expansion and creep property changes induced by changes in temperature could be included in the mechanical response. Since temperature and stress gradients occur in different regions, the thermal and structural calculations required mesh refinement in different areas. As a result, the thermal and structural finite element meshes used for the Room B calculation were different, and nodal temperatures computed using the Aria calculation were interpolated to the nodes of the structural mesh (Fig. 2). The interpolation code MAPVAR (Wellman 1999) was used to perform this task.

The thermal model was constructed assuming all external boundaries were adiabatic, and that the entire formation was prescribed to have an initial temperature of 300 K. The configuration remained at 300 K for the first 324 days and then the thermal load of 1.8 kW per canister was applied to the finite element model at the appropriate location. The discrete thermal loading from each of the canisters was simulated two-dimensionally as a uniform line source located on the left symmetry plane, extending from a depth of 3.37 m below Clay G to 5.96 m below Clay G. The thermal load for each canister was distributed over the canister spacing of 1.52 m and canister height of 2.59 m to give a uniform heat flux of 456 W/m^2 condition on the symmetry plane, only half of this load or 228 W/m^2 was applied to the thermal finite element model. A thirty year half life was simulated with a decaying exponential such that the therma1 load applied along the length of the heat source had the form:

$$q = 228 \exp\left(-7.327 \times 10^{-10} t\right) \tag{15}$$

where q is the thermal load in W/m^2 and t is the time in seconds. The thermal properties of all stratigraphic materials were assumed to be the same as those for halite. This assumption was appropriate because earlier work had shown that thermal responses using both an all-salt stratigraphy and a layered stratigraphy were essentially the same (see Argüello et al., in prep. for additional details). Heat transfer through the salt was modeled with a nonlinear thermal conductivity of the form:

$$\lambda = \lambda_{300} \left(300 / T\right)^{\gamma} \tag{16}$$

where λ is the thermal conductivity, T is the absolute temperature in Kelvin, and λ_{300} and γ are material constants. The excavated room (i.e., WIPP Room B) was treated as an "equivalent thermal material" with a conductivity allowing radiation heat transfer in the room to be simulated by conduction. This approximate method of modeling radiation was used in the WIPP Benchmark II numerical simulation activity (Morgan et al. 1981), and the properties of the "equivalent thermal material" were chosen so that the thermal response computed with this material is almost the same as the response computed by modeling radiation in the room. Note that the "equivalent thermal material" was not included in the structural model mesh. The thermal properties of halite and the "equivalent thermal material," used in this simulation are presented in Table 2.

Table 2. Thermal properties used in Room B thermal simulations using Aria.

Material		Halite	"Equivalent thermal material"
Density, ρ (kg/m^3)		2300	1
Specific heat, c_p (J/kg/K)		860	1000
Coefficient of linear thermal expansion, α (K^{-1})		45×10^{-6}	N/A
Thermal conductivity parameters	λ_{300} (W/m/K)	5	50
	γ	1.14	0

The halite thermal property values were taken from the original WIPP reference property set, as described by Krieg 1984, for halite and the properties for the "equivalent thermal material" are the same as those used in Benchmark II (Morgan et al. 1981). Lastly, the thermal loss from the room was modeled by a convective boundary at the WIPP room B surfaces using Newton's law of cooling as:

$$q' \bullet n = h(T - 300) \tag{17}$$

where q' is the thermal flux vector, n is the outward normal unit vector, h is the convective heat transfer coefficient, and T is the surface temperature in Kelvin. The convective boundary acts as a heat sink whenever the temperature on the room surface exceeds the initial 300 Kelvin temperature. Thus, as the room surface temperature rises, the rate of heat loss increases. Because the convective heat transfer coefficient was unknown, it was adjusted prior to any structural calculations until a suitable value (0.18 W/m^2/K) was determined to give agreement with the measured temperatures reported above and below the WIPP Room B, similar to what was done in the historical calculation.

With the exception of some material properties and the fact that the model is now subjected to heat loading, the mechanical computational model for Room B is, for all practical purposes, almost identical to the model used for Room D. It has been described in the previous sub-section and will not be repeated here. Only the subtler differences are discussed, including the behavior of the non-salt materials. The anhydrite and polyhalite regions are now modeled as separate materials, as was done in the historical calculation of Munson et al. 1990a. The anhydrite and polyhalite materials are modeled using a Drucker-Prager constitutive model to treat elastic and inelastic behavior. The mechanical responses of the anhydrite and polyhalite materials were treated elastically until yielding occurs, but once the yield stress is reached, plastic strain accumulates. The Drucker-Prager criterion can be written as:

$$\sqrt{J_2'} = c - aI_1 \tag{18}$$

where $\sqrt{J_2'}$ is the second deviatoric stress invariant, c & a are constants, and I_1 is the first stress invariant. Values of c=1.35 MPa and a=0.45 were used for the anhydrite and c=1.42 MPa and a=0.473 were used for the polyhalite in the Room B calculation. In addition, the value of the MD Model parameter, K_0, previously used for argillaceous halite in Room D has now also been modified, as was also done in the historical calculation. A value of $K_0=1.783\times10^6$ is used for the Room B argillaceous halite material.

2.3.3 *Thermal and closure results from SIERRA Mechanics*

In the interest of brevity, only a few results from the Room B calculation are presented here to illustrate the validity of SIERRA Mechanics for this class of problems. Many more details on this calculation, as well as for the isothermal Room D calculation, can be found elsewhere (Argüello et al., in prep.).

Figure 3 shows the computed thermal response for a series of six points extending from immediately adjacent to the roof of the room up some distance vertically into the host rock, as indicated by the numbers in parenthesis shown in the legend of the figure, where these numbers, 15.2, 9.1, etc., are in units of meters. These locations correspond to measurement locations probed by the B_745 thermocouple unit (Munson et al. 1990b). It is apparent that, in general, the agreement between calculation and data is better closer to the room surface. However, even for the outermost locations, the agreement is still relatively good, with only a few degrees difference.

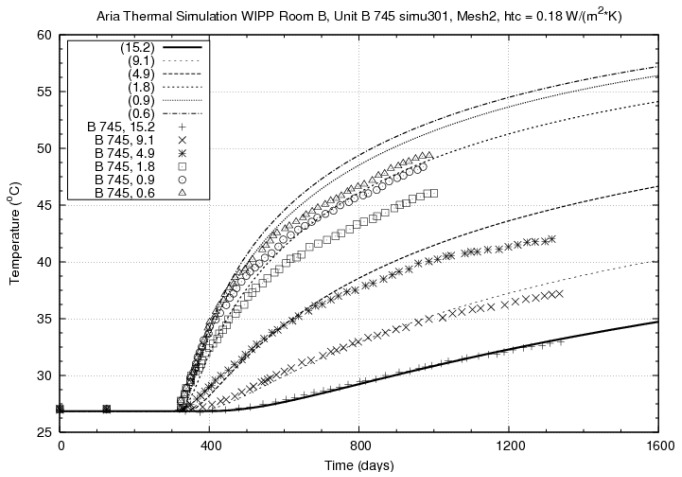

Figure 3. Comparisons of measured in-situ Room B temperatures from thermocouple unit B_745 with computed results from SIERRA Mechanics.

Similarly, Figure 4 shows the computed thermal response for a series of points extending from immediately adjacent to the floor of the room down some distance off-vertically into the host rock, per the numbers in parenthesis shown in the legend of the figure. These locations correspond to measurement locations probed by the B_706 thermocouple unit (Munson et al. 1990b). At these locations, the agreement between calculation and data is quite good overall. This general trend, of acceptable agreement, pervaded throughout the other thermocouple units where comparisons were made, with agreement at some locations better than at others.

Figure 5 shows the room closure results from the thermo-mechanical simulation compared to the extensometer measurements of Room B closure, measured at room midwidth and midheight. Again, in view of the complexity of the calculation, the agreement between calculation and measurement is quite good, with an under-prediction of horizontal and vertical closures of less than 1% and approximately 14%, respectively, at 1000 days. This is roughly the same order as the agreement seen in the historical calculation of Munson et al. (1989), and once again, in a preliminary sense, validates SIERRA Mechanics for non-isothermal conditions to roughly the same degree as was done for the codes used in the historical calculation. It should be noted that, from their historical calculation, Munson et al. (1990a) thought that "the large discrepancy between the calculated and measured vertical closure is believed to be a direct consequence of fracture and separation in the immediate roof." Because the MD model, as presented above, is not capable of modeling those features, we concur with their assessment and believe that such capability, among others, should be pursued in any future advanced salt constitutive model developed for incorporation into SIERRA Mechanics for modeling the next generation of repository systems in salt.

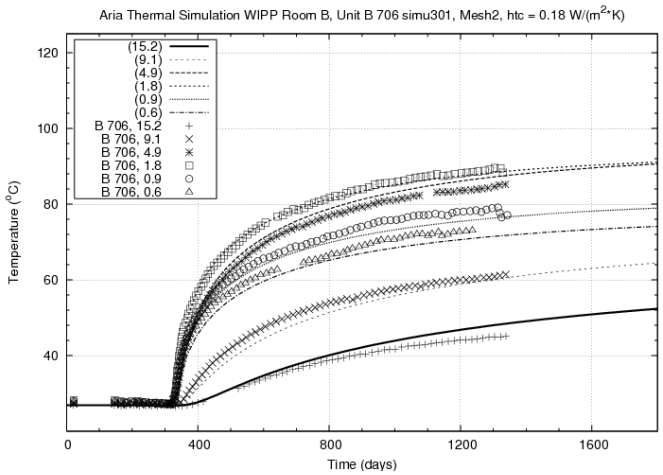

Figure 4. Comparisons of measured in-situ Room B temperatures from thermocouple unit B_706 with computed results from SIERRA Mechanics.

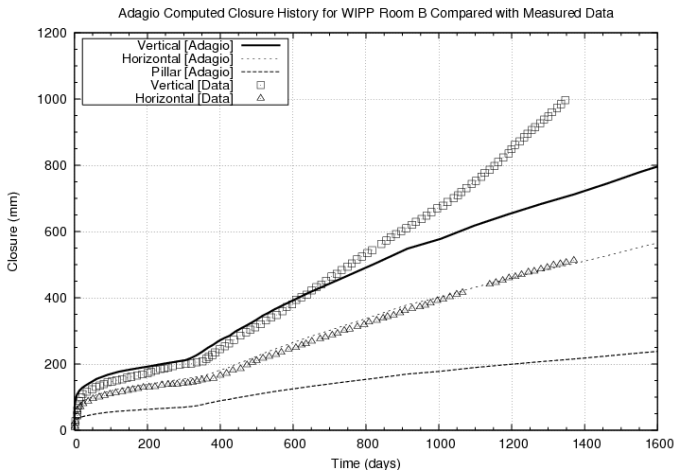

Figure 5. Comparison of measured in-situ Room B closures with computed results from SIERRA Mechanics.

3 LARGE 3D DEMONSTRATION PROBLEM

A scoping study was recently performed of a generic salt repository (GSR) for disposal of wastes generated by a conventional spent nuclear fuel recycling facility (Stone et al. 2010). Because the in-situ tests discussed previously are relatively small computational problems it was desirable to demonstrate the SIERRA Mechanics toolset applied to a more challenging computational model of a more realistic size that could be more typical of the problem size that will need to be solved for future repository systems. Furthermore, although complex, the previously described in-situ thermal-mechanical problem only exercised the code suite in a one-way coupled mode and it was desirable to demonstrate that the toolset can solve more fully coupled-physics problems. Finally, it was also desirable to demonstrate the SIERRA Mechanics capability on a truly 3D configuration, typical of what will be needed in next-generation tools applied to a repository setting.

The GSR study proposed a disposal strategy in which a series of panels is constructed underground. Each panel consists of individual rooms, with each room containing many alcoves. The disposal strategy assumes placement of one waste package at the end of each alcove, to be covered by crushed salt backfill for radiation-shielding of personnel accessing adjacent alcoves. The backfill effectively insulates the waste package, locally increasing waste package and near-field repository temperatures. The thermal output for each of the vitrified borosilicate glass waste canisters is 8,400 W with decay to approximately 30% original power output at 50 years.

A coupled thermal-mechanical analysis of the salt repository was performed using the SIERRA

Mechanics code suite. The goals of the analysis were to determine the peak intact salt temperature over time and to characterize the closure response of the alcove including the change in porosity of the crushed salt backfill. A 3D finite element model of a single storage alcove and haulage-way was developed utilizing planes of symmetry through the alcove and adjacent haulage-way. Two different analysis domains and mesh discretizations were utilized; one for the thermal analysis and a different discretization for the geomechanics analysis. Figure 6 shows a close-up of the mesh used for the geomechanical analysis. Field transfer operators in the SIERRA toolkit were used to pass interpolated nodal temperature and displacement data between the different (thermal and mechanical) domains. This simulation was run using 96 processors and took approximately 96 hours per processor to complete compared to less than ten of hours on a single processor for the in-situ test calculations described earlier.

Some of the discriminating features of this highly nonlinear thermal-mechanical analysis included the use of thermal contact surfaces to model the effect of room closure on the thermal conduction that occurs as the room surfaces deform and come into contact. The mechanical effect of the large salt creep deformation was also captured through the use of contact surfaces in the mechanical calculation. The effect of thermal radiation between heated surfaces within the alcove and haulage-way was also modeled within SIERRA Mechanics using the capability to recompute the radiation view factors as the surfaces deform. Unlike in the previous in-situ test calculations, the use of an "equivalent" material for thermally modeling the room was not needed. The mechanical response of the salt was modeled using both a Norton power law secondary creep model and the MD model described earlier. The compaction behavior of the crushed salt backfill was modeled with a nonlinear pressure versus volume-strain relationship.

The details of this simulation, as well as results of both the thermal and mechanical analyses, are presented in Stone et al. 2010. Here we include only select results that demonstrate the complex three-dimensional room-closure behavior. The need for the large deformation, large strain mechanics formulation is clearly shown by the magnitude of the deformation (Fig. 7). The crushed salt backfill develops a non-uniform porosity with most of the compaction occurring near the roof of the alcove (Fig. 8). This variation of compaction of the backfill from higher at the roof to lower near the floor is in qualitative agreement with some measurements of porosity in the backfill seen in the BAMBUS field experiments.

4 SUMMARY & CONCLUSIONS

Herein, results from a systematic study have been presented in which the SIERRA Mechanics code suite was exercised on a set of salt repository problems, including the isothermal Room D and the heated Room B in-situ experiments at the WIPP. This was done to validate its applicability to this class of problems and to further demonstrate its use on anticipated more-complex coupled simulations of future nuclear waste salt repositories.

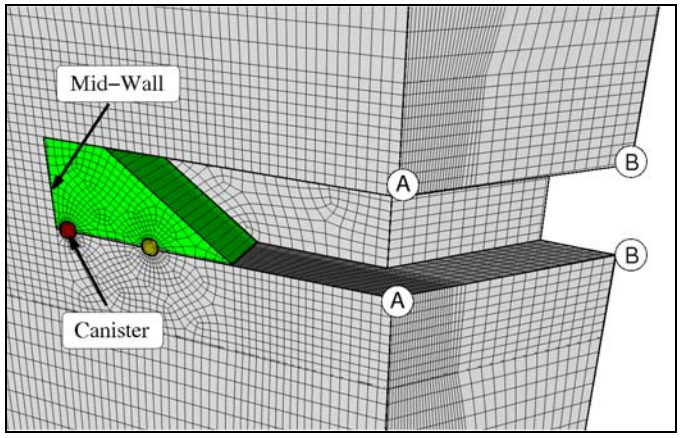

Figure 6. Schematic showing the location of points at the alcove and access tunnel corners.

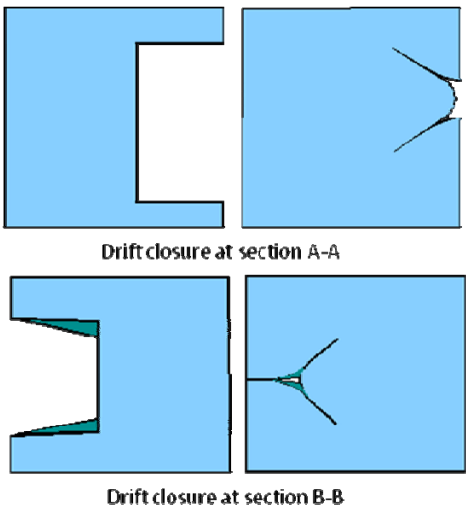

Figure 7. Un-deformed and deformed views of the access tunnel looking from the back of the model toward the alcove/access-tunnel intersection (upper) and vice-versa (lower).

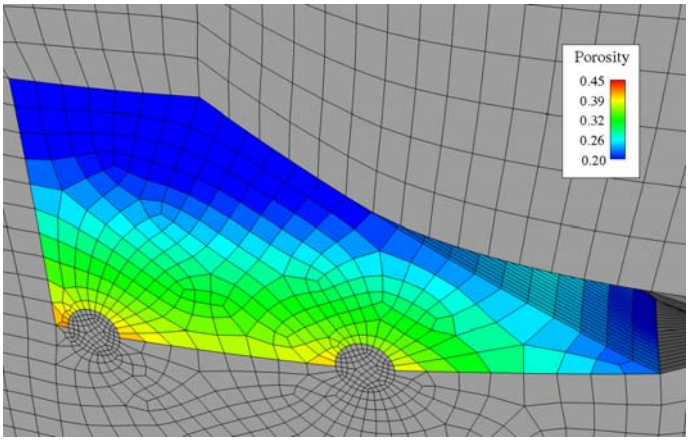

Figure 8. Porosity in the crushed salt backfill at 8 years for the MD model simulation with an initial emplaced porosity of 42%.

Results shown indicate that, in view of the complexity of the calculations used for the two in-situ experiments, the agreement between the SIERRA Mechanics calculations and measurements is quite good, roughly the same order as the agreement seen previously in the historical calculations. Therefore, in a preliminary sense, these two simulations of in-situ experiments at the WIPP validate SIERRA Mechanics to roughly the same degree as has been done previously. However, modern verification & validation (V&V) and uncertainty quantification (UQ) practices are likely to place significantly more stringent requirements on such computational tools to deem them acceptable, in a regulatory sense, for future nuclear waste repositories in salt.

The demonstration GSR calculation has shown the applicability of SIERRA Mechanics to large-scale parallel computational problems that are likely to be the norm in assessing future repositories. This code suite is an example of a valuable toolset for use on the NEAMS Waste IPSC project or, at least, one with the capabilities that can be developed as the disposal community ventures into the next generation of repository computational tools.

ACKNOWLEDGEMENTS

We wish to acknowledge James Bean for his many contributions to this effort, John Holland for his contributions on the GSR calculation, and the DOE NE NEAMS program for supporting this work. Sandia National Laboratories is a multi-program laboratory managed and operated by Sandia Corporation, a wholly owned subsidiary of Lockheed Martin Corporation, for the U.S. Department of Energy's National Nuclear Security Administration under contract DE-AC04-94AL85000.

REFERENCES

Argüello, J. G., Wang, Y., Freeze, G. A., Davison, S. M., Jove-Colon, C. F., Lee, J. H., Mariner, P., Rath, J. S., & Siegel, M. 2011. Nuclear Energy Advanced Modeling and Simulation (NEAMS) Waste Integrated Performance and Safety Codes (IPSC): Fiscal Year 2011 Progress Report. SAND2011-XXXX, Sandia National Laboratories, Albuquerque, NM (in prep.).

Edwards, H. C., & Stewart, J. R. 2001. SIERRA: A Software Environment for Developing Complex Multi-Physics Applications. In K. J. Bathe (ed.), *First MIT Conference on Computational Fluid and Solid Mechanics*. Amsterdam: Elsevier.

Freeze, G., Argüello, J. G., Howard, R., McNeish, J., Schultz, P. A., & Wang, Y. 2010. Challenge Problem and Milestones for: Nuclear Energy Advanced Modeling and Simulation (NEAMS) Waste Integrated Performance and Safety Codes (IPSC). *SAND2010-7175, Sandia National Laboratories*. Albuquerque, NM.

Freeze, G., Argüello, J. G., Bouchard, J., Criscenti, L., Dewers, T., Edwards, H. C., Sassani, D., Schultz, P. A., & Wang, Y. 2011. Nuclear Energy Advanced Modeling and Simulation (NEAMS) Waste Integrated Performance and Safety Codes (IPSC): FY10 Development and Integration. *SAND2011-0845, Sandia National Laboratories*. Albuquerque, NM.

Krieg, R. D. 1984. Reference Stratigraphy and Rock Properties for the Waste Isolation Pilot Plant (WIPP) Project. *SAND83-1908, Sandia National Laboratories*, Albuquerque, NM.

Matalucci, R. V., Christensen, C. L., Hunter, T. O., Molecke, M. A., & Munson, D. E. 1984. Waste Isolation Pilot Plant (WIPP) Research and Development Program: In Situ Testing Plan, March 1982. *SAND81-2628, Sandia National Laboratories*, Albuquerque, NM.

Morgan, H. S., Krieg, R. D., & Matalucci, R. V, 1981. Comparative Analysis of Nine Structural Codes Used in the Second WIPP Benchmark Problem. *SAND81-1389, Sandia National Laboratories*, Albuquerque, NM.

Munson, D.E. 1979. Preliminary Deformation-Mechanism Map for Salt (with Application to WIPP). *SAND70-0079, Sandia National Laboratories*, Albuquerque, NM.

Munson, D.E. & Dawson, P.R. 1979. Constitutive Model for the Low Temperature Creep of Salt (With Application to WIPP). *SAND79-1853, Sandia National Laboratories*, Albuquerque, NM.

Munson, D.E. & Dawson, P.R. 1982. A Transient Creep Model for Salt during Stress Loading and Unloading. *SAND82-0962, Sandia National Laboratories*, Albuquerque, NM.

Munson, D.E. & Dawson, P.R. 1984. Salt Constitutive Modeling using Mechanism Maps. *Proc. 1st International Confe-*

rence on the Mechanical Behavior of Salt, Clausthal-Zellerfeld: Trans Tech Publications.

Munson, D.E., Fossum, A.F., & Senseny, P.E. 1989. Advances in Resolution of Discrepancies between Predicted and Measured in Situ WIPP Room Closures. *SAND88-2948, Sandia National Laboratories*, Albuquerque, NM.

Munson, D. E., Jones, R. L., Hoag, D. L., & Ball, J. R. 1988. Mining Development Test (Room D): In Situ Data Report (March 1984 - May 1988) Waste Isolation Pilot Plant (WIPP) Thermal/Structural Interactions Program. *SAND88-1460, Sandia National Laboratories*, Albuquerque, NM.

Munson, D. E., DeVries, K. L., & Callahan, G. D. 1990a. Comparison of calculations and in situ results for a large, heated test room at the Waste Isolation Pilot Plant (WIPP). In Hustrulid & Johnson (ed.), *Rock Mechanics Contributions and Challenges, Proc. 31st U. S. Symposium on Rock Mechanics*. Rotterdam: Balkema.

Munson, D. E., Jones, R. L., Ball, J. R., Clancy, R. M., Hoag, D. L., & Petney, S. V. 1990b. Overtest for Simulated Defense High-Level Waste (Room B): In Situ Data Report (May 1984 - February 1988) Waste Isolation Pilot Plant (WIPP) Thermal/Structural Interactions Program. *SAND89-2671, Sandia National Laboratories*, Albuquerque, NM.

Notz, P. K., Subia, S. R., Hopkins, M. M., Moffat, H. K., & Noble D. R. 2007. Aria 1.5: User Manual. *SAND2007-2734, Sandia National Laboratories*, Albuquerque, NM.

SIERRA Solid Mechanics Team. 2010. Adagio 4.18 User's Guide. *SAND2010-6313, Sandia National Laboratories*, Albuquerque, NM.

Stone, C. M., Holland, J. F., Bean, J. E., & Argüello, J. G. 2010. Coupled Thermal- Mechanical Analyses of a Generic Salt Repository for High-Level Waste (ARMA-10-180). *Proc. American Rock Mechanics Association (ARMA) 44th US Rock Mechanics Symposium, 27-30 June 2010.* Salt Lake City: American Rock Mechanics Association.

Wellman, G. W. 1999. MAPVAR - A Computer Program to Transfer Solution Data Between Finite Element Meshes. *SAND99-0466, Sandia National Laboratories*, Albuquerque, NM.